

**\*\*Volume Title\*\***

*ASP Conference Series, Vol. \*\*Volume Number\*\**

**\*\*Author\*\***

© **\*\*Copyright Year\*\*** *Astronomical Society of the Pacific*

## Phase-lag Distances of OH Masing AGB Stars

D. Engels,<sup>1</sup> S. Etoka,<sup>1</sup> E. Gérard<sup>2</sup> and A. Richards<sup>3</sup>

<sup>1</sup>*Hamburger Sternwarte, Universität Hamburg, Germany*

<sup>2</sup>*Galaxies, Étoiles, Physique et Instrumentation (GEPI), Observatoire de Paris, Meudon, France*

<sup>3</sup>*Jodrell Bank Centre for Astrophysics, Department of Physics and Astronomy, University of Manchester, UK*

**Abstract.** Distances to AGB stars with optically thick circumstellar shells cannot be determined using optical parallaxes. However, for stars with OH 1612 MHz maser emission emanating from their circumstellar shells, distances can be determined by the phase-lag method. This method combines a linear diameter obtained from a phase-lag measurement with an angular diameter obtained from interferometry. The phase-lag of the variable emission from the back and front sides of the shells has been determined for 20 OH/IR stars in the galactic disk. These measurements are based on a monitoring program with the Nançay radio telescope ongoing for more than 6 years. The interferometric observations are continuing. We estimate that the uncertainties of the distance determination will be  $\sim 20\%$ .

### 1. Introduction

In the final phases of AGB evolution, the mass-loss rate increase is such that the star is partially obscured in the visual and even near infrared bands, as the circumstellar envelope (CSE) gets optically thick. It is assumed that this occurs mostly for intermediate mass stars ( $M > 2 M_{\odot}$ ), but direct evidence is lacking, at least for the Galactic disk, because of uncertainty in the distances.

Distances to obscured AGB stars cannot be determined using optical parallaxes; however, the maser emission shown by many OH/IR stars can be used. Parallax measurements of post-AGB stars and Mira variables were successfully made using H<sub>2</sub>O (Imai et al. 2007) and OH masers (Vlemmings & van Langevelde 2007), but have not been attempted for OH/IR stars so far. Another promising way to obtain reliable distances is the measurement of the phase-lag between the varying peaks of the OH maser emission. This yields the absolute linear diameter of the shell and, in combination with the angular diameter of the shell measured in interferometric maps, gives the distance (Herman & Habing 1985; van Langevelde et al. 1990). The OH/IR stars usually exhibit maser spectra dominated by two peaks with a separation of  $30 \pm 10 \text{ km s}^{-1}$ . This double-peak characteristic can be explained if the maser emission comes from a rather thin, uniformly expanding shell. The strongest masers then originate from the front and the back sides of the shell. The stars are often large-amplitude variable stars, and the maser flux density follows these regular variations. Due to the light travel time through the CSE, the observer sees the peak from the back side of the shell responding with a delay  $\tau_0$  relative to the peak on the front side. These delays are of the order of weeks.

With the Nançay Radio Telescope (NRT) we monitored a sample of 20 OH/IR stars to measure their phase-lags. For about half of the sample, phase-lags had been determined by Herman & Habing (1985) and van Langevelde et al. (1990). Some of the stars served as comparison stars to verify the reported phase-lags. For others a re-determination was the goal, as the reported phase-lags were inconsistent with each other. For the remaining stars, phase-lags were determined for the first time. We have also started to image stars at 1612 MHz with the eVLA and e-MERLIN near maximum light to determine the angular diameters. We report here on the status of the program and give preliminary results.

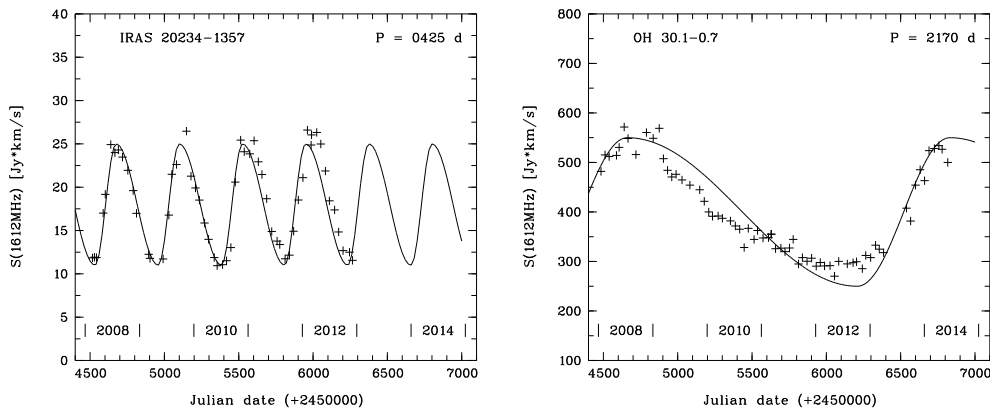


Figure 1. Sample light curves of the OH maser flux integrated over the full velocity profile for IRAS 20234–1357 ( $P = 1.16$  yr) and OH 30.1–0.7 ( $P = 5.95$  yr).

## 2. Light Curves and Phase-lag Determinations

The sample of OH/IR stars was observed with the NRT in the 1612 MHz OH maser line once every month over 5 years (2008–2012). For several sources with insufficient coverage of the variation cycle, the monitoring is continuing. Typical integration times on source were 5–10 minutes, yielding a typical noise level of 100 mJy. The spectra were baseline fitted and calibrated (nominal error  $\sim 5\%$ ) and have a velocity resolution of  $0.035\text{--}0.070$  km s $^{-1}$ . Representative light curves of the integrated flux are shown in Figure 1. All stars are large-amplitude variables with periods  $P \approx 1 - 6$  years. The light curves are smooth with some month-to-month scatter. This scatter is not due to secular variations of individual maser features in the spectral profile, superposed on the smooth variation of the flux integrated over all features. Indeed, dividing spectra of adjacent months showed that any variations affected the full profile, and not individual features only. We therefore conclude that the month-to-month scatter is dominated by calibration errors.

The light curves of objects with periods  $< 2$  years are well represented by a sine curve, except that the level of maximum light is not necessarily recovered in each cycle. The light curves become increasingly asymmetric with longer periods, with a steeper rise towards maximum (duration  $0.3 - 0.4 \cdot P$ ) and a gentle decline towards minimum. Simple analytical functions, such as an asymmetric sine function, are not able to reproduce the detailed shapes of these light curves.

To find the phase-lag  $\tau_0$  between the front- and back-side emission (corresponding to the blue and red parts of the maser velocity profile), we assumed that the maser light curves of both velocity ranges are similar, e.g. they differ only in mean flux and amplitude. For all sources, the peak flux densities of the two maser peaks were always  $\gg 1$  Jy, so that all parts of the light curves were sampled with high signal-to-noise ratio. The phase-lags were then determined by minimizing the function  $\Delta F = F_r(t) - a \cdot F_b(t + \tau_0) + c$ , where  $F_b, F_r$  are the integrated fluxes over the blue and red parts of the velocity profile, and  $a$  and  $c$  are constants to match amplitude and mean flux of the two maser features. An example is shown in Figure 2 for the OH/IR star OH 16.1–0.3, which has one of the longest periods in the sample: 6.03 years. In this case the uncorrected light curves show an apparently smaller phase-lag in the rising part of the light curve and a larger lag in the declining part. This case shows that full coverage of a variation cycle is essential to determine amplitude and mean flux correctly before the phase-lag is determined. The resulting phase-lag of  $100 \pm 10$  days is more than twice as large as the value, 38.3 days, measured by van Langevelde et al. (1990), although their period of  $P = 6.2$  years is in good agreement with ours.

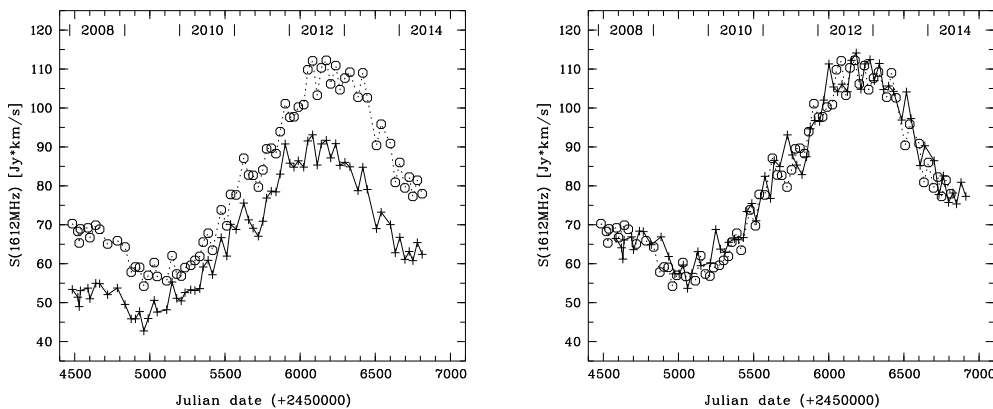


Figure 2. *Left:* Light curves of the maser emission integrated over the blue part ( $[-3; +21]$  km s $^{-1}$ ; crosses) and the red part ( $[+21; +45]$  km s $^{-1}$ ; circles) of the velocity profile of OH 16.1–0.3 ( $P = 6$  yrs). *Right:* Best match of the light curves after scaling and shifting the blue light curve and applying a phase-lag  $\tau_0 = 100$  days.

### 3. Improved Angular Diameters

The determination of the angular diameter in principle requires imaging the OH maser shell at tangential velocities, e.g. in the center of the velocity interval, where the emission is faint. Because this emission is hard to detect, the diameters are usually determined by extrapolation of the projected diameters at non-tangential velocities assuming that the masers reside in a thin radially symmetric shell. We are currently observing the stars interferometrically, close to the maxima of their light curves, to detect as much as possible from the faint tangential emission. The aim is to improve the angular diameters derived from less sensitive observations in the past, to determine diameters for stars not imaged at 1612 MHz so far, and to derive constraints on deviations from radial symmetry of the shells.

OH 16.1–0.3 is one of the objects we observed with the eVLA, and which had not previously been imaged at 1612 MHz. The interferometric observations were obtained in November 2011 with a velocity resolution of  $0.69 \text{ km s}^{-1}$ . Calibration, following the relevant steps for observations taken in spectral-line mode, and final imaging were performed with CASA (Common Astronomy Software Application). A sensitivity of  $2 \text{ mJy beam}^{-1}$  per channel was reached. The restoring beam size was  $(1''.95 \times 1''.0)$  with a position angle  $\text{PA} \approx -28^\circ$ . Figure 3 presents, in the right panel, the integrated emission over the red inner wings of the spectra covering the velocity range  $[+25; +37] \text{ km s}^{-1}$ , which gives the best rendering of the diameter of the shell, and a typical spectrum of the source at the left. The shell is roughly circular with a possible hint of an elongated streak of material in the south east of the shell.

The best fit (by eye) of the projected shell diameter is given by the magenta circle of  $\sim 3''.43$  diameter. Correcting for the projection effect assuming a thin shell, the full angular diameter of the shell is  $\phi = 4''.1 \pm 0''.6$ . In combination with the linear diameter  $d_{\text{OH}} = (1.73 \pm 0.17)10^4 \text{ AU}$  corresponding to the phase-lag of 100 days, the distance to OH 16.1–0.3 is  $D = 4.2 \pm 0.7 \text{ kpc}$ .

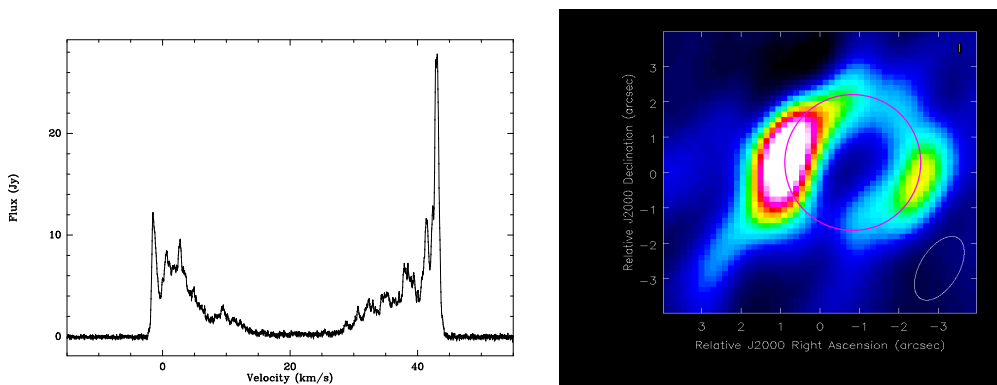


Figure 3. *Left:* NRT spectrum of OH 16.1–0.3. *Right:* Integrated emission over the red inner part of the spectrum of OH 16.1–0.3 covering the velocity range  $[+27; +37] \text{ km s}^{-1}$ . The magenta circle presents the best fit of the projected diameter of the shell.

#### 4. Results and Conclusions

Preliminary results of the observing program of the full sample are summarized in Table 1. Given are the object name, the newly determined period  $P$ , the linear diameter  $d_{\text{OH}}$  (in AU)  $= 0.1731 \cdot \tau_0$  (in days) calculated from the phase-lag  $\tau_0$ , the angular diameter  $\phi$ , and the distance  $D$ . Uncertainties are  $< 3\%$  for the periods  $P$  and approximately  $20\%$  for the linear diameters  $d_{\text{OH}}$ .  $P$  and  $d_{\text{OH}}$  are taken from the NRT observations, while the angular diameters of the shell are taken from the literature (Amiri et al. 2012; Baud 1981; Chapman et al. 1984; Herman et al. 1985; Norris et al. 1982; Wolak et al. 2013), except for OH 16.1–0.3 (eVLA) and for OH 83.4–0.9 (e-MERLIN), which come from our own recent observations.

The shell diameters cover a range of  $\sim 2000 - 17000 \text{ AU}$ , and in general the diameters are larger for longer periods. The angular diameters taken from the literature can be rather uncertain, depending on the degree of extrapolation applied to derive the full

extent of the shells. An obvious case is OH 141.7+3.5, where the angular diameter provided by Chapman et al. (1984) is strongly underestimated, yielding an unreasonably great distance. The accuracy of the distances currently is not better than 20%, where this uncertainty reflects only the uncertainty of the phase-lag determination.

Table 1. Results from the OH 1612 MHz monitoring program.

Object	$P$ [yr]	$d_{\text{OH}}$ [ $10^3$ AU]	$\phi$ [ $''$ ]	$D$ [kpc]	Object	$P$ [yr]	$d_{\text{OH}}$ [ $10^3$ AU]	$\phi$ [ $''$ ]	$D$ [kpc]
20234–1357	1.16	< 1.7			OH 32.0–0.5	4.16	11.2	1.07	10.6
OH 44.8–2.3	1.47	2.6	2.6	1.0	OH 127.8+0.0	4.36	9.5	2.69	3.6
IRC +50137	1.74	1.7			OH 26.5+0.6	4.36	6.0	4.49	1.4
01037+1219	1.78	4.3	8.0	0.5	OH 75.3–1.8	4.52	10.4		
05131+4530	2.88	5.2			OH 32.8–0.3	4.63	10.4	2.74	3.8
OH 39.7+1.5	3.45	2.9	4.0	0.7	OH 20.7+0.1	4.71	15.6	1.65	9.4
OH 55.0+0.7	3.48	8.6			OH 104.9+2.4	4.79	6.0	2.88	2.1
21554+6204	3.51	5.2			OH 30.1–0.7	5.95	10.4	2.69	3.9
OH 138.0+7.2	3.86	1.7	0.8	2.2	OH 16.1–0.3	6.03	17.3	4.10	4.2
OH 83.4–0.9	4.11	5.2	~1.8	~3.0	OH 141.7+3.5	6.05	13.0	0.76	17.1:

For eleven stars of the sample, phase-lags (linear shell diameters) are available from van Langevelde et al. (1990). Within our estimated uncertainty of 20% we obtained agreement for OH 26.5+0.6, OH 32.0–0.5, OH 44.8–2.3 and OH 104.9+2.4. For the remaining sources, as in the case of OH 16.1–0.3, higher deviations were found. OH 127.8+0.0 was monitored by Wolak et al. (2013) between 2002 and 2008, also with the NRT. They determined a period of 1600 days and a phase-lag of 62 days, which is in perfect agreement with our results ( $P = 1590$  days and  $\tau_0 = 55$  days).

We expect that the linear shell diameters can be determined with an error  $\sim 10\%$ , by analyzing the variations of the phase-lag across the velocity profile (see Wolak et al. 2013), instead of using the integrated fluxes. In addition, the uncertainties in the distances will depend on the deviations from radial symmetry of the shells. Assuming that these deviations do not exceed 10% (Etoka & Diamond 2010), the uncertainties in the distances should not exceed 20%. This will be probed by the interferometric observations, which are expected to continue until 2017.

## References

- Amiri, N., Vlemmings, W. H. T., Kemball, A. J., & van Langevelde, H. J. 2012, *A&A*, 538, A136
- Baud, B. 1981, *ApJ*, 250, L79
- Chapman, J., Cohen, R. J., Norris, R. P., Diamond, P. J., & Booth, R. S. 1984, *MNRAS*, 207, 149
- Etoka, S., & Diamond, P. J. 2010, *MNRAS*, 406, 2218
- Herman, J., Baud, B., Habing, H. J., & Winnberg, A. 1985, *A&A*, 143, 122
- Herman, J., & Habing, H. J. 1985, *A&AS*, 59, 523
- Imai, H., Sahai, R., & Morris, M. 2007, *ApJ*, 669, 424
- Norris, R. P., Diamond, P. J., & Booth, R. S. 1982, *Nature*, 299, 131
- van Langevelde, H. J., van der Heiden, R., & van Schooneveld, C. 1990, *A&A*, 239, 193
- Vlemmings, W. H. T., & van Langevelde, H. J. 2007, *A&A*, 472, 547
- Wolak, P., Szymczak, M., & Gérard, E. 2013, *MNRAS*, 430, 2499

**Discussion**

*Whitelock:* Very nice results. Do you have accurate luminosities from the mid-infrared to go with the distances?

*Engels:* Bolometric fluxes can be obtained nowadays between 2 and 200  $\mu\text{m}$  by various IR surveys. Combining them with the phase-lag distances gives a range of 5000 – 50 000  $L_{\odot}$ , consistent with a classification as intermediate-mass stars at the very end of AGB evolution.

*Olofsson:* If your stars are in the super-wind phase, it appears to me that you find much larger durations of this phase than the ones obtained from dust studies (see Lombaert's presentation).

*Engels:* The masers are pumped by photons emitted in the superwind at much smaller distances from the stars than the masers themselves. The masers might be located at distances where the dust and gas is from the pre-superwind phase.